

Three-dimensional modelling of the DC glow discharge using the second order fluid model

Abstract. This paper presents the development of a three dimensional second order fluid model, used to properly describe a DC glow discharge, maintained by secondary emission at cathode, at low pressure, by using Cartesian geometry. The transport description of the charged species uses the corresponding first three moments of Boltzmann equation, coupled in a self-consistent way with Poisson equation. Some assumptions are required in order to simplify the numerical procedure. Thus, all transport equations are treated in the same manner, using classical drift-diffusion expression for fluxes. We used in this work, the Tchebychev distribution for the longitudinal positions, which gives dense grids near the electrodes in order to accurately resolve the sheaths and to speed up the computing time.

Streszczenie. W artykule zaprezentowano trójwymiarowy model opisujący DC wyładowanie jarzeniowe otrzymywane przez emisję katodowa przyt niskim ciśnieniu. Do opisu wykorzystano równanie Boltzmann sprężone z równaniami Poissona. (Trójwymiarowe modelowanie wyładowania jarzeniowego DC przy użyciu modelu cieczy drugiego rzędu)

Keywords: DC Glow Discharge, 3D Cartesian geometry, Fluid Model, Tchebychev Distribution

Słowa kluczowe: wyładowanie jarzeniowe, model cieczy, rozkład Czebyszewa

Introduction

Low pressure glow discharges are of topical interest for lots of technological applications like plasma light sources and plasma processing in the microelectronics industry, such as etching and deposition of thin films [1]. Because of their importance, there has been growing efforts to understand the glow discharge mechanisms and to simulate the discharge processes. Therefore, a three-dimensional description of the macroscopic characteristics of the DC glow discharge in the Argon-like gas is presented in this paper. Such work is motivated by the development of complex numerical models in the last decade which are readily solvable using computers available nowadays.

The set of fluid equations considered in this work for modelling a glow discharge in three dimensions should be regarded as a pure macroscopic representation of the Boltzmann equation whose solution concerns mainly the calculation of the electron and ion densities and the electron energy. The electric field and plasma potential are given by Poisson equation. To resolve the self-consistent continuum modelling equations in one and two dimensions, many numerical models were proposed during the last years. In our three-dimensional model we use the time splitting method, such method consists in replacing the three-dimensional equations by a system of one-dimensional equations [4]. The discretization for longitudinal positions used in this work is the Chebyshev distribution.

Modelling equations

The model used to describe the kinetics of the charged particles for the low pressure glow discharge is the second order fluid model. It is based on the first three moments resolution of the Boltzmann equation. These three moments are continuity, momentum transfer and energy equations, which are strongly coupled with the Poisson's equation by considering the local mean energy approximation, in which, one supposes that the function of distribution is completely determined by the density and local average energy electronic or ionic. This assumption, of local balance can be used as relation of closing the transport equations system.

The self-consistent continuum modelling equations consists of four partial differential equations and their associated boundary conditions: Poisson's equation, electron and ion continuity equations and the electron energy balance. These equations can be solved for potential field, electron and ion number densities, and electron temperature. Electric field strengths, particle fluxes,

and ionization rates may then be computed as secondary quantities from these solutions.

The three-dimensional equations of the electron and positive ion density in Cartesian geometry can be written as:

$$(1) \quad \frac{\partial n_e(\vec{r}, t)}{\partial t} + \frac{\partial \Phi_e(\vec{r}, t)}{\partial \vec{r}} = S(\vec{r}, t)$$

$$(2) \quad \frac{\partial n_p(\vec{r}, t)}{\partial t} + \frac{\partial \Phi_p(\vec{r}, t)}{\partial \vec{r}} = S(\vec{r}, t)$$

With $\vec{r}(x, y, z)$ is the position vector

In the source term, only the ionization is considered, and other reactions are neglected, because we think that ionization is the main process in the glow discharge [2]. As the production of ion–electron pairs is caused by energetic electrons, the ionization rate is proportional to the number density of electrons n_e as well as the number density of the neutral particles N which can be ionized.

The source term $S(\vec{r}, t)$ is expressed as a function of the electron temperature T_e in an Arrhenius form as shown [3].

$$(3) \quad S(\vec{r}, t) = k_i N n_e(\vec{r}, t) \exp(-E_i / K_b T_e(\vec{r}, t))$$

Where: k_i is the pre-exponential coefficient, E_i is the ionization activation energy and K_b is the Boltzmann constant.

In the model, Electron and ion momentum transport equations are reduced to the classical drift-diffusion expression of the fluxes:

$$(4) \quad \Phi_e(\vec{r}, t) = -n_e(\vec{r}, t) \mu_e E(\vec{r}, t) - D_e(\vec{r}, t) \frac{\partial n_e(\vec{r}, t)}{\partial \vec{r}}$$

$$(5) \quad \Phi_p(\vec{r}, t) = n_p(\vec{r}, t) \mu_p E(\vec{r}, t) - D_p(\vec{r}, t) \frac{\partial n_p(\vec{r}, t)}{\partial \vec{r}}$$

The Electron diffusivity temperature dependent is given by the following expression:

$$(6) \quad D_e(\vec{r}, t) = \mu_e \frac{K_b T_e(\vec{r}, t)}{e}$$

The electron temperature is calculated by the energy electron equation given by:

$$(7) \quad \frac{\partial n_e(\vec{r}, t)}{\partial t} + \frac{5}{3} \frac{\partial \Phi_e(\vec{r}, t)}{\partial \vec{r}} = S_e(\vec{r}, t)$$

Where: $n_\varepsilon(\vec{r}, t) = n_e(\vec{r}, t) \varepsilon_\varepsilon(\vec{r}, t)$ is the electron energy density.

The flux of electron energy density can be written as:

$$(8) \quad \Phi_\varepsilon(\vec{r}, t) = -\frac{5}{3} (n_\varepsilon(\vec{r}, t) \mu_e E(\vec{r}, t) + D_e(\vec{r}, t) \frac{\partial n_\varepsilon(\vec{r}, t)}{\partial \vec{r}})$$

In the energy source term given by:

$$(9) \quad S_\varepsilon(\vec{r}, t) = -e\Phi_e(\vec{r}, t)E(\vec{r}, t) - S(\vec{r}, t)H_i$$

An Ohmic heating term $e\Phi_e(\vec{r}, t)E(\vec{r}, t)$ and a collision loss term $S(\vec{r}, t)H_i$ in ionization are encountered, in which H_i is the ionization enthalpy loss.

The electrical discharge potential is given by resolving Poisson equation:

$$(10) \quad \frac{\partial^2 V(\vec{r})}{\partial \vec{r}^2} = \frac{e}{\varepsilon_0} (n_e(\vec{r}, t) - n_p(\vec{r}, t))$$

The electric field can be denoted as the negative gradient of the potential:

$$(11) \quad E(\vec{r}, t) = -\frac{\partial V(\vec{r})}{\partial \vec{r}}$$

Boundary conditions

Fluid equations as well as Poisson's equation can be solved only if boundary conditions are specified.

For Poisson's equation, the boundary conditions include the fact that the anode is grounded ($V_{anode} = 0$) and that a negative voltage $V_{cathode} = -V_{DC}$ is applied to the cathode.

For fluid equations the boundary conditions at the grounded electrode ($x=0$) are given as follow:

$$\begin{aligned} n_e(\vec{r}, t) &= 0 \\ \nabla n_p(\vec{r}, t) &= 0 \\ \frac{5}{2} \nabla T_e(\vec{r}, t) - \frac{e}{K} \nabla V(\vec{r}) &= 0 \end{aligned}$$

And at the powered electrode ($x = X_{max}$):

The secondary electron emission by ion bombardment at the cathode constitutes the most important process. It is described by the relation of the electron and ion flux.

$$(12) \quad \Phi_e(\vec{r}, t) = -\gamma \Phi_p(\vec{r}, t)$$

Therefore, the relation (12) is used as boundary condition at the cathode for the electron equation.

$$\begin{aligned} \nabla n_p(\vec{r}, t) &= 0 \\ T_e(\vec{r}, t) &= T_{ec} \end{aligned}$$

For symmetry reasons at the reactor axis ($y=0$) and ($z=0$), the Neumann's conditions are used in our 3D simulation for electrical potential, electron and ion densities and also for electron energy.

We assume that the recombination of the charged particles on the wall is immediately completed and the conductivity of perfect dielectric [4]. Consequently, we suppose that the values of the electron and ion densities on the dielectric walls ($y=Y_{max}$) and ($z=Z_{max}$) are zero ($n_e(\vec{r}, t) = 0$ and $n_p(\vec{r}, t) = 0$)

The boundary conditions used in our model are recapitulated in Fig.1 below:

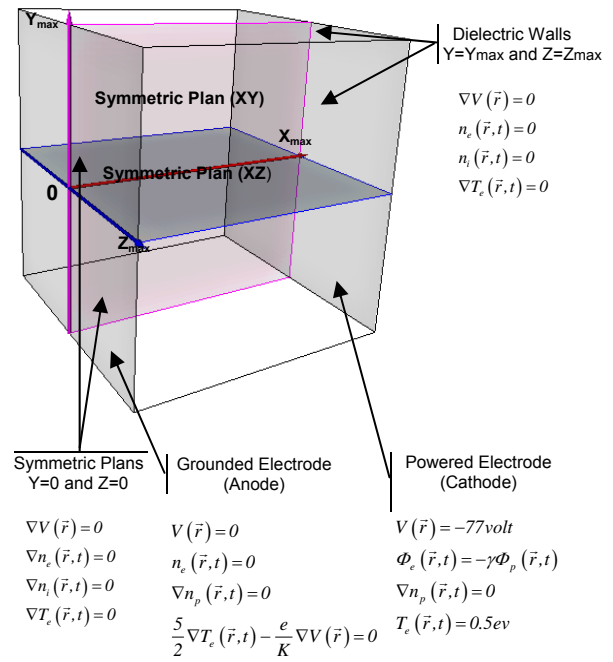


Fig.1. Three-dimensional Cartesian DC discharge geometry used for the simulation

Numerical methods

For the charged particles, continuity type equations (1) and (2) have to be solved. The transport equation for electron energy (7) has the same form, by changing particle density $n_e(\vec{r}, t)$ with electron mean energy density $n_\varepsilon(\vec{r}, t)$ and correctly expressing the source term $S_\varepsilon(\vec{r}, t)$. Thus the resolution of the transport equations is done in the same way.

Thus the form of the transport equation to be solved is expressed as follows:

$$(13) \quad \frac{\partial n}{\partial t} + \frac{\partial \Phi}{\partial x} + \frac{\partial \Phi}{\partial y} + \frac{\partial \Phi}{\partial z} = S$$

In this work, we use the method of the fractional steps [5] to solve the equation (13). This method consists in replacing the three-dimensional equations by a system of one-dimensional equations in the object to reduce considerably the calculation time in each direction of space.

$$(14.a) \quad \frac{\partial n}{\partial t} = S$$

$$(14.b) \quad \frac{\partial n}{\partial t} + \frac{\partial \Phi}{\partial x} = 0$$

$$(14.c) \quad \frac{\partial n}{\partial t} + \frac{\partial \Phi}{\partial y} = 0$$

$$(14.d) \quad \frac{\partial n}{\partial t} + \frac{\partial \Phi}{\partial z} = 0$$

The discretization method of the equations of the system above is based on the finite difference scheme.

Theoretically, any discretization grid can be employed. However, the solutions are much more precise with a smaller discretization step, therefore of a high number of points, which increases the computing time. To avoid this problem, we use in this paper the Tchebychev distribution for the longitudinal positions which gives dense grids near the electrodes in order to accurately resolve the sheaths.

$$(15) \quad x_i = \frac{1}{2} \left(\cos\left(\frac{(i-1)\pi}{M-1}\right) + 1 \right), \quad i = M, M-1, \dots, 1$$

The system of equations becomes:

$$(16.a) \quad \frac{n_{i,j,k}^{m+1} - n_{i,j,k}^m}{\Delta t} = S_{i,j,k}$$

$$(16.b) \quad \frac{n_{i,j,k}^{m+1} - n_{i,j,k}^m}{\Delta t} + \frac{\Phi_{i+1/2,j,k} - \Phi_{i-1/2,j,k}}{\Delta x_i} = 0$$

$$(16.c) \quad \frac{n_{i,j,k}^{m+1} - n_{i,j,k}^m}{\Delta t} + \frac{\Phi_{i,j+1/2,k} - \Phi_{i,j-1/2,k}}{\Delta y} = 0$$

$$(16.d) \quad \frac{n_{i,j,k}^{m+1} - n_{i,j,k}^m}{\Delta t} + \frac{\Phi_{i,j,k+1/2} - \Phi_{i,j,k-1/2}}{\Delta z} = 0$$

with: $\Delta x_i = x_{i+1/2} - x_{i-1/2}$

The drift-diffusion fluxes are discretized using the Scharfetter-Gummel exponential scheme [6].

$$(17) \quad \Phi_{i+1/2,j,k} = \frac{D_{i+1/2,j,k}}{\Delta x^+} \left(\frac{R_1}{1 - \exp(R_1)} n_{i+1,j,k} - \frac{R_1 \exp(R_1)}{1 - \exp(R_1)} n_{i,j,k} \right)$$

$$(18) \quad \Phi_{i-1/2,j,k} = \frac{D_{i-1/2,j,k}}{\Delta x^-} \left(\frac{R_2}{1 - \exp(R_2)} n_{i,j,k} - \frac{R_2 \exp(R_2)}{1 - \exp(R_2)} n_{i-1,j,k} \right)$$

where:

$$R_1 = \mu_{i+1/2,j,k} \frac{E_{i+1/2,j,k}}{D_{i+1/2,j,k}} \Delta x^+$$

$$R_2 = \mu_{i-1/2,j,k} \frac{E_{i-1/2,j,k}}{D_{i-1/2,j,k}} \Delta x^-$$

$$\Delta x^- = x_i - x_{i-1}$$

$$\Delta x^+ = x_{i+1} - x_i$$

After the substitution of the exponential scheme for the flux, the discretized continuity equation (16) has the form of a three-point equation for the density; Which need to be solved at every time step Δt .

Many numerical techniques exist for the solution of such sets of three-point equations, varying in their efficiency and simplicity. In this work, we used the Thomas algorithm to calculate the density $n_{i,j,k}^{m+1}$.

Solving the Poisson equation is usually one of the most expensive parts of simulations of density models for glow discharge. The Poisson's equation is most often discretized in a 3D Cartesian grid by using central finite-difference scheme.

$$(20) \quad \Delta V(x, y, z) = \frac{\partial^2 V}{\partial x^2} + \frac{\partial^2 V}{\partial y^2} + \frac{\partial^2 V}{\partial z^2}$$

$$\text{With: } \begin{cases} \frac{\partial^2 V}{\partial x^2} = 2 \frac{\Delta x^+ V_{i-1,j,k} - (x_{i+1} - x_{i-1}) V_{i,j,k} + \Delta x^- V_{i+1,j,k}}{(x_{i+1} - x_{i-1}) \Delta x^+ \Delta x^-} \\ \frac{\partial^2 V}{\partial y^2} = \frac{V_{i,j-1,k} - 2 V_{i,j,k} + V_{i,j+1,k}}{\Delta y^2} \\ \frac{\partial^2 V}{\partial z^2} = \frac{V_{i,j,k-1} - 2 V_{i,j,k} + V_{i,j,k+1}}{\Delta z^2} \end{cases}$$

The resulting linear system is then solved using iterative methods from the Successive Over-Relaxation (SOR) family [7].

Results and discussions

The self-sustained solutions of the governing equations for the three-dimensional model that we described above with a direct current (DC) exciting source are presented in this paper. The discharge gas is chosen to be argon-like for neutral temperature $T = 323 \text{ }^\circ\text{K}$. It is assumed that a parallel plate configuration is used for the glow discharge simulation with equal area electrodes (10.16×10.16) cm^2 ,

and the electrode separation distance, 3.525 cm as shown in Fig. 1. The transport parameters have been taken from [8]. The step of discretization is supposed to be variable in the longitudinal direction.

The following table gathers all the source data and the transport parameters used in our three-dimensional modelling.

Table.1. Gas physical properties and glow discharge system physical dimensions [8]

Symbol	Value
X_{max}	3.525 cm
Y_{max}	5.08 cm
Z_{max}	5.08 cm
N	$2.83 \times 10^{16} \text{ cm}^{-3}$
μ_e	$2 \times 10^5 \text{ cm}^2 / \text{V} \cdot \text{sec}$
μ_p	$2 \times 10^3 \text{ cm}^2 / \text{V} \cdot \text{sec}$
D_p	$10^2 \text{ cm}^2 / \text{sec}$
E_i	24 eV
H_i	15.578 eV
γ	0.046
V_{DC}	77.4 V
T_{ec}	0.5 eV
k_i	$2.5 \times 10^{-6} \text{ cm}^3 / \text{sec}$

In order to validate and test the developed numerical model in this work for the simulation of the DC glow discharge in 3D geometry, we carried out a study of this discharge under the same conditions of simulation of Lin and Adomaitis [8]. Then, we compared our results 3D represented along the symmetric axis ($y = 0$ and $z = 0$) in 1D with those obtained by Lin and Adomaitis.

The results of the test of validity of the macroscopic discharge characteristics such as the charged particle densities, plasma potential and electron temperature are represented in the figs. 2, 3, 4 and 5, which show clearly a very good agreement between the results obtained from our numerical code on the symmetric axis of the reactor and those given by Lin and Adomaitis.

Both sheaths and bulk phases characterizing glow discharge can be seen in the particle number density profiles (see figs. 2, 3). The density inside the sheath is much lower than that of the bulk phase, where the net space charge is negligible following the ambipolar approximation.

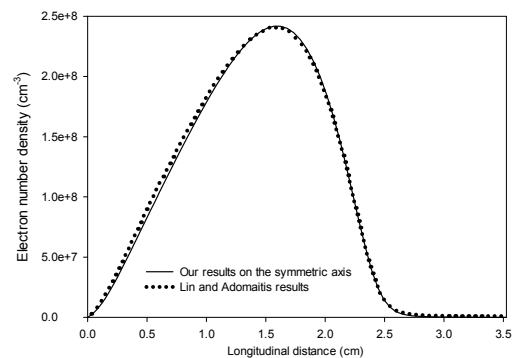


Fig. 2: Electron density on the symmetric axis

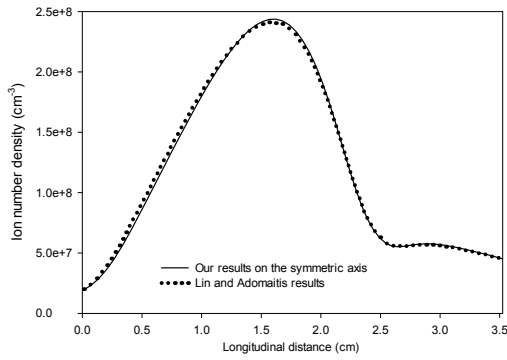


Fig. 3: Ion density on the symmetric axis

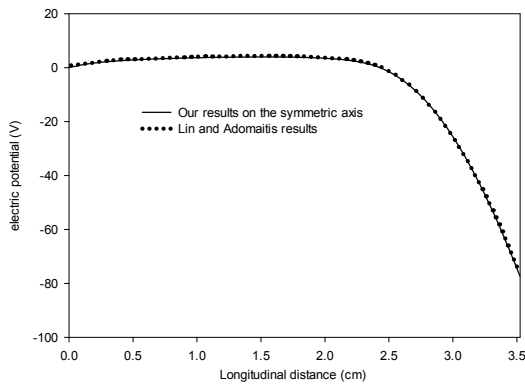


Fig. 4: Electric potential on the symmetric axis

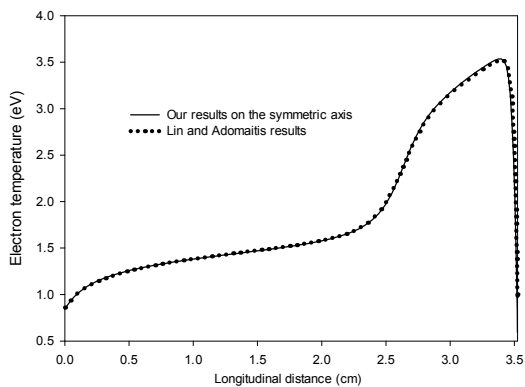


Fig. 5: Electron temperature on the symmetric axis

Fig. 5 is the plot of the of the electron temperature on the symmetric axis. The considerable increase of the temperature near the cathode is due to the high gradient of potential in this area (see fig. 4). The electron cooling is due to the ionization reactions, which are highly endothermic, then, the small drop of the temperature near the anode is due to the electrons moving against the electric field.

From the results obtained above, on the symmetric axis, we can say that our three-dimensional numerical model is able to describe correctly the electrical and physical properties of the DC glow discharge, object of our study. For better comprehension of the dynamics of the charged particles and to easily observe the compoment of the glow discharge, we present hereinafter, the 3D plot of its main electrical characteristics. In order to allow a clear view of the evolution of the discharge in the center of the reactor; Each characteristic is represented by two figures: the first

indexed (a) shows the plot of the complete 3D profile and the second indexed (b) is a plot of the half profile, cut on the level of the tangential symmetric plan ($z = 0$).

We note that all the results presented in this paper are taken at the stationary state of the discharge which is obtained after 0.8×10^{-3} s in our case.

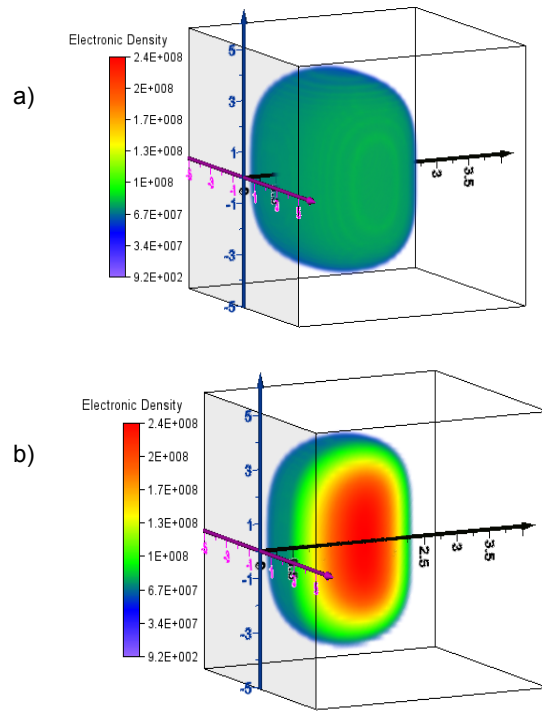


Fig. 6: 3D Electron density (cm^{-3})

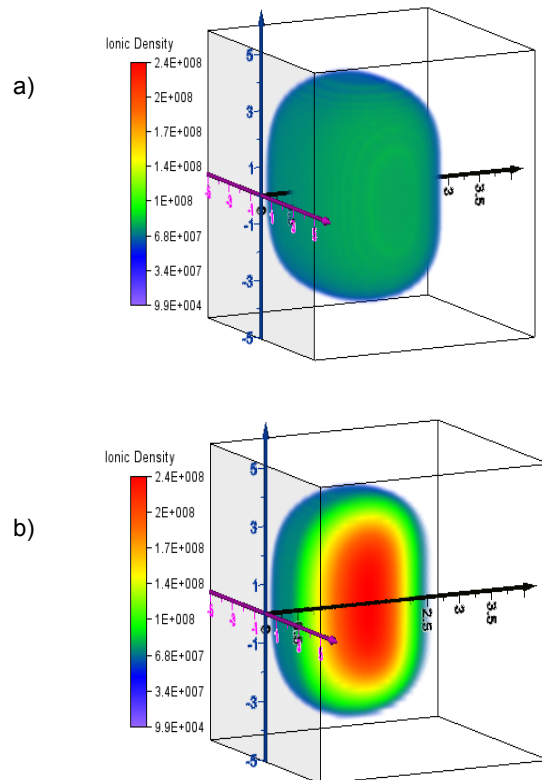


Fig. 7: 3D Ion density (cm^{-3})

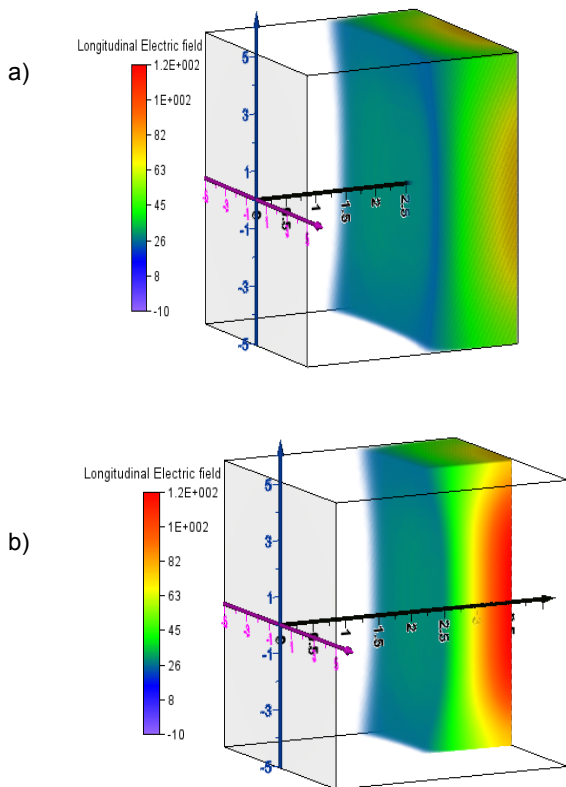


Fig. 8: 3D Longitudinal electric field (V.cm⁻¹)

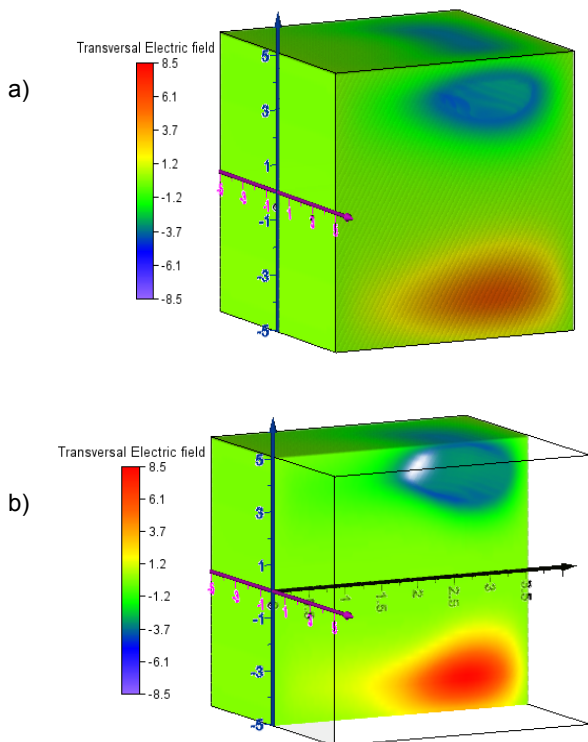


Fig. 9: 3D Transversal electric field (V.cm⁻¹)

Figs. 6 and 7 contain the 3D spatial distributions of the electron and ion densities. Maximum density both for electrons and ions reaches $2.4 \times 10^8 \text{ cm}^{-3}$. The electron density decreases significantly in the anode sheath and cathode fall with respect of the volume, the white zone corresponding to a very low density compared to the

maximum in the bulk region (smaller than $9.2 \times 10^2 \text{ cm}^{-3}$ for electron and $9.9 \times 10^4 \text{ cm}^{-3}$ for ion). The density in the sheath, however, cannot be treated as zero because the sheath region is the source of the particle generation by secondary emission process. Zero density here means no reactions.

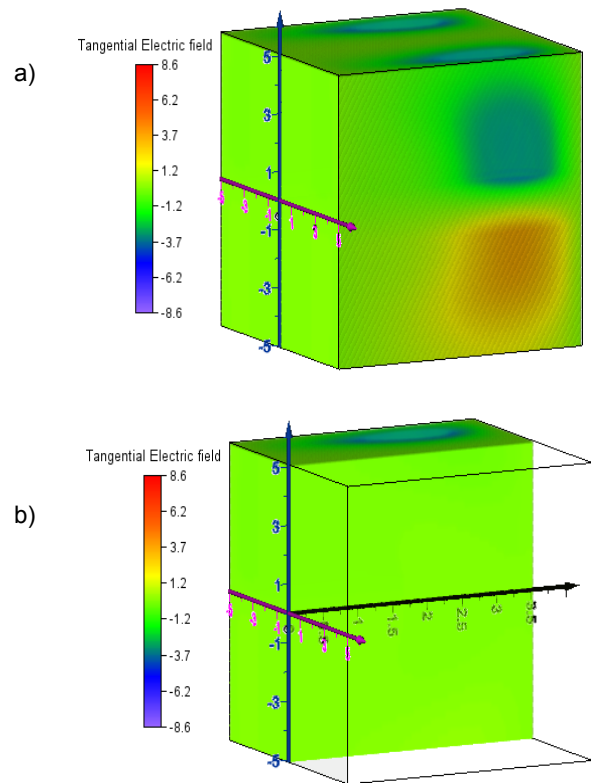


Fig. 10: 3D Tangential electric field (V.cm⁻¹)

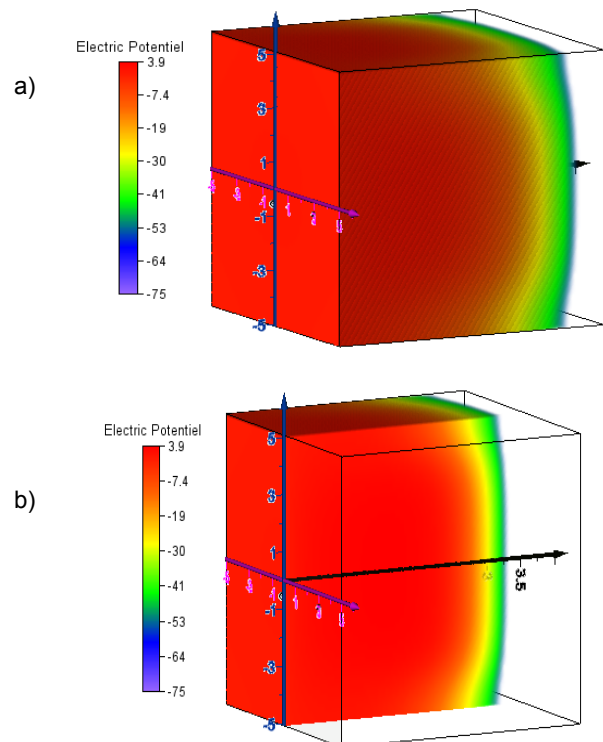


Fig. 11: 3D electric potential (V)

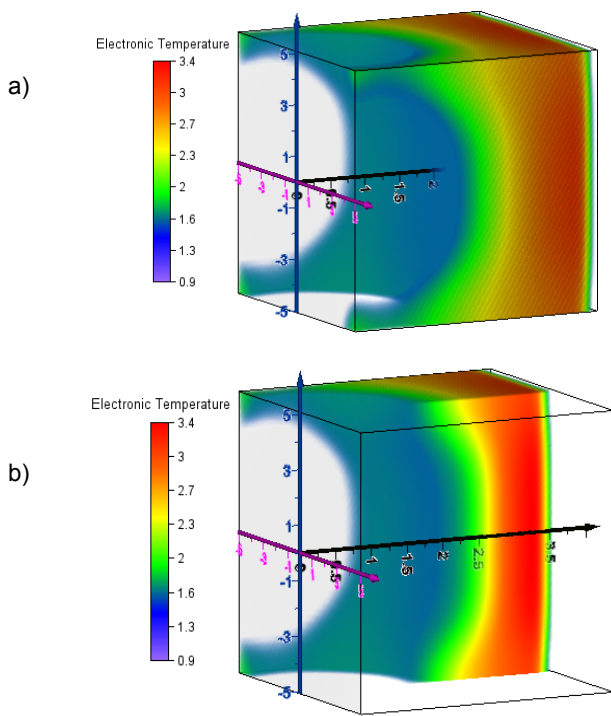


Fig. 12: 3D Electron temperature (eV)

Fig. 8 is the plot of the 3D longitudinal component of the electric field. The electric field strength at both electrodes is nonzero and it is much greater at the cathode than at the anode because of the potential gradient; thus ions bombard both electrode surfaces and with greater intensity at the powered electrode. The field is almost zero in the positive column because the potential is almost unvaried (see fig.11).

Figs. 9 and 10 represent the three-dimensional spatial dependence of the transversal and tangential components of the electric field respectively; these components present asymmetric distributions with respect to the symmetry axis ($y=0$ and $z=0$). Due to this fact, the resulting of the transversal and tangential components of the electric field are almost zero in the inter-electrodes gap. The main role of these components is to maintain the glow discharge confined around the symmetry axis.

We can see the 3D profile of expected electron temperature in fig. 12, which confirms our 1D result on the symmetric axis presented in fig. 5. Generally, the spatial distribution of the electronic temperature follows the variations of the electric field

Conclusion

In this paper, we have developed a three-dimensional model of the glow discharge being maintained by a term source of electrons and ions uniformly produced by a secondary electron emission at the cathode.

The algorithm based on finite difference method coupled to the time splitting technical is a good approach to resolve three-dimensional transport equation of the glow discharge model at low pressure. Our calculations in the symmetry axis of glow discharge are in good agreement with the 1D work of Lin and Adomatis [8].

Nomenclature

n_e, n_p and n_e	Electron, ion and energy number density
Φ_e, Φ_p	Electron and Ion flux

S	Source term for Electron and Ion
V	Electric potential
E	Electric field
ϵ_e	Electron energy
T_e	Electron temperature
μ_e, μ_p	Electron and Ion Mobility
D_e, D_p	Electron and ion diffusivity
γ	Coefficient for secondary electron emission
N	Neutral species density
e	Elementary charge
ϵ_0	Free space permittivity
X_{\max}	Longitudinal inter-electrode gap
Y_{\max}	Transversal inter-electrode gap
Z_{\max}	Tangential inter-electrode gap
Δx	Longitudinal spatial step
Δy	Transversal spatial step
Δz	Tangential spatial step
Δt	Temporal step

REFERENCES

- [1] Rafatov I.R., Akbar D., Bilikmen S., Modelling of non-uniform DC driven glow discharge in argon gas, *Physics Letters A* 367 (2007), 114–119
- [2] Yu Qian, Deng Yong Feng, Numerical study on characteristics of argon radio-frequency glow discharge with varying gas pressure, *Chin.Phys.Lett.* Vol. 25(2008), No. 7, 2569
- [3] Elghazaly M.H., Solyman S., Electron impact ionization and excitation rate coefficients in the negative glow region of a glow discharge, *Journal of Quantitative Spectroscopy & Radiative Transfer* 103 (2007), 260–271
- [4] Kraloua B., Hennad A., Multidimensional numerical simulation of glow discharge by using the N-BEE-Time splitting method, *Plasma Science and Technology*, Vol.14, Sep(2012), No.9
- [5] Hundsdorfer W., Portero L., A note on iterated splitting schemes, *Journal of Computational and Applied Mathematics*, 201(2007), 146-152
- [6] L. Scharfetter, H. K. Gummel, *IEEE Trans. Electron Devices*, 64(1969), No.16
- [7] Luque A., Ebert U., Density models for streamer discharges: Beyond cylindrical symmetry and homogeneous media, *Journal of Computational Physics* 231 (2012) 904–918
- [8] Yi-hung Lin, Raymond A. Adomaitis, A global basis function approach to DC glow discharge simulation, *Physics letters*, A 243 (1998), 142-150

Authors

Hocine Tebani was born in Tissemsilt, Algeria, on April, 12, 1980. His scientific interests include the theoretical study and modeling of physical processes in gas discharge plasma. E-mail: hocinetebani@yahoo.fr

Ali Hennad was born in Oran, Algeria, on January, 27, 1964. He received the PH.D degree with a thesis on the kinetics of ions in molecular gases to determine ion basic data in air form Monte Carlo simulation, University Paul Sabatier of Toulouse, France in 1996. He is currently a Professor at University of Sciences and Technology of Oran, Algeria. His field of expertise is more particularly the modeling of the electric and hydrodynamic behaviors of the plasmas generated in low and high pressure. He has also a good expertise on the numerical analysis of the nonlinear and strongly coupled elliptic transport equations, and the swarm parameters determination of the charged particles in no equilibrium reactive plasma. He is the author of various international publications, a lot of them in collaboration with the LAPLACE Laboratory, Toulouse, France. E-mails: ali_hennad@yahoo.fr